Imperial College London

Department of Physics

The role of the cosmological constant in gravitational lensing

by

CID: 00919977

Project code: ASTR-Heavens-1

Supervisor: Prof. Alan Heavens

Assessor: Prof. Carlo Contaldi

Word count: 8256

Acknowledgements

I wish to thank my supervisor Prof. Alan Heavens for his guidance and support through this project. I would also like to extend special thanks to Pierre Fleury, whom I've never met, for writing the paper that clearly laid out some of the important mathematics to get me started on light propagation in the Swiss-cheese, without whom I would have been stuck for much longer.

Abstract

There is an ongoing debate in the literature about whether the cosmological constant Λ directly affects gravitational lensing. In this work we place this problem in a Swiss-cheese model with a Kottler vacuole, and numerically integrate null geodesics in this model to investigate the influence of Λ on observable quantities in lensing. Our numerical results are compared with the predictions from conventional lensing analysis, Rindler and Ishak (2007), and Kantowski et al. (2010), and we find that the numerical results agree best with Kantowski's predictions. However, it is difficult to isolate the influence of Λ since it would necessarily change either the density or curvature of the FRW universe, both of which affect the propagation of light in a Swiss-Cheese universe. Nevertheless, our results estimate the effect of Λ to be of the order of 10^{-6} or less, which is smaller than the second order mass terms commonly neglected in gravitational lensing analysis.

Contents

1 Introduction

1.1 Motivation and background

It has been established that the Universe is accelerating in its expansion, based on various complementary observations (Riess et al., 2004; Spergel et al., 2003). In the ΛCDM cosmological model, this acceleration is powered by a cosmological constant Λ that dominates the Universe's current energy budget. Ironically, the idea of a cosmological constant was first pioneered by Einstein, who introduced the term to keep his equations static, but later dropped it when evidence showed otherwise. As fate would have it, the cosmological constant has made its way back into modern cosmology to account for the accelerating expansion of the Universe. Empirically, there is an onslaught of past cosmological data Carmeli and Kuzmenko (2001), de Bernardis et al. (2000), and Peebles and Ratra (2003) that our universe has a small but positive cosmological constant.

An active dispute that has been the subject of several papers in the last decade is whether and consequently, how the cosmological constant affects the deflection of light. It is well known that light traveling through space is bent according to the mass distribution it encounters in an effect known as gravitational lensing. This phenomenon forms one of the important observational cornerstones of General Relativity (Will, 1993). Since its first discovery in the 1970s, gravitational lensing has grown into one of the most deeply investigated phenomenon of gravitation and is becoming an increasingly important tool for observational astrophysics and cosmology.

Given the undisputed success of General Relativity, and the central role that Λ now plays in gravitational physics, one would think that the effect of a cosmological constant on gravitational lensing is well understood. However, this is not the case. Scientific opinion is divided on this issue and till now, there is still no consensus as to whether Λ contributes directly to lensing. Debate persists on whether the conventional gravitational lensing formalism is already sufficient. Despite this, there is general agreement that the influence of the cosmological constant on the bending of light, if any, is relatively small. However, cosmological measurements are becoming more precise and the possibility of next-generation applications of lensing as a tool for cosmology only render the hanging debate more pressing. If the influence of the cosmological constant on light deflection is found to be different from the current prevalent expectation, future lensing observations will have to take this

difference into account, and observations could very well allow for a new and independent constraint on Λ.

Therefore, though perhaps not of immediate practical significance, the question of whether or how Λ contributes to gravitational lensing is a debate that deserves to be settled. With this work we hope to shed some light on this dispute.

1.2 Previous work

We are concerned about whether Λ directly contributes to the bending of light around a concentrated mass. It is important to note that classical lensing already takes into account an implicit dependence on Λ through the use of angular diameter distances, which will be explained in detail in Chapter 2. This is a Λ effect that is known and already taken care of; therefore, when debating about whether Λ contirbutes directly to lensing, we are really asking whether any modification to the current lensing formalism involving Λ is needed.

Conventional view, first put forth by Islam (1983), is that no such modification is necessary, and classical lensing is correct as it is. This view, supported later by multiple authors (Lake, 2002; Park, 2008; Simpson et al., 2010; Khriplovich and Pomeransky, 2008), argues that the equations describing the path followed by a photon, the null geodesic equations, are independent of Λ and therefore the photon trajectory is wholly unaffected by the presence of a cosmological constant. This has been the official opinion up until about a decade ago.

The main challenge to the conventional view came from Rindler and Ishak (2007), who argue that while Λ drops out of the equations of motion, it still affects light bending through the metric of spacetime itself, since the photon is moving in Λ-dependent geometry. Physical measurable angles are defined by the metric, and since the spacetime metric itself includes a comological constant, the process of measurement causes the cosmological constant to creep into the light bending angle.

Since then, a plethora of papers have been written about this topic, but none have conclusively settled the debate. While there have been supporting arguments in favour of Rindler and Ishak's proposal (Sereno, 2008; Schücker, 2008; Bhadra et al., 2010), more recently there have been several arguments against it that question whether the influence of the cosmological constant has already been taken into account in the angular diameter distances and impact parameter in the formula (Arakida and Kasai, 2012; Butcher, 2016; Piattella, 2016). A large portion of the conflict comes from the fact that coordinate angles are not necessarily physically measurable—indeed, most of the disagreements are about how the mathematical results should translate into observable quantities, especially since the pioneering analyses use a static metric that does not take into account the relative movement of the observer and source.

To date, most of the work done on this topic has been analytical. This inevitably lend some of the work to criticisms of whether the approximations used in deriving the results are valid (see for example criticisms in Ishak, Rindler, and Dossett (2010)). There has been some numerical work on this subject, but they are few and far from comprehensive. For example, Beynon (2012) adopted the use of a Lemaître-Tolman-Bondi metric to model an overdensity in an expanding background and numerically integrated null geodesics in this model, but did not reach a definitive conclusion. More recently (Aghili et al., 2017) used the McVittie metric (McVittie, 1933) in analyzing the effect of Λ.

The closest related work was done by Schücker (2009), who adopted a partially numerical approach in the model we are using (the Swiss-cheese model) and concluded he agrees with Rindler and Ishak, but he only uses a single numerical example to reach a conclusion. Furthermore, some higher-order terms were dropped out in the integration in the Kottler metric and the contribution of Λ to the deflection was not singled out. He compares the results of *different* models (pure Kottler versus Swiss-cheese), both involving a non-zero Λ, to observed quantities. Hence his result are more inclined towards answering the question of which is the right physical model for gravitational lensing, as compared to the question we hope to answer, which is: What is the influence of the cosmological constant given a *single* model, which we assume for the purpose of the analysis, and not without basis, is an accurate model of our universe? On this note we take a slightly different approach from Schücker, where we work with one model (the Swiss-cheese), and compare the results from a $\Lambda = 0$ universe with a universe in which we have a non-zero Λ.

Our work will be numerical, and we hope to tackle some of the shortcomings of the previous numerical work, without falling into the approximation traps that exist in analytical work. In addition, we use a Swiss-cheese model that deals with the problem of comoving observers in a cosmological setting and we use observable quantities throughout to compare the effect of Λ. The details of the model will be explained further in Chapter 3.

1.3 Structure of this report

In the next chapter I give an introduction of General Relativity and the basics of light propagation, which lays the mathematical foundation for this work. Following that, I provide an overview of the current established literature on gravitational lensing in a Schwarzschild spacetime where $\Lambda = 0$ and derivation of the key equations, before moving on to the case of a non zero Λ.

The bulk of the work is in Chapter 3, where I give the mathematical derivation of the equations which form the basis of this project, some of which do not appear explicitly in literature. In particular, I describe the construction and mathematical properties of the Swiss-cheese model with a Kottler condensation, and based on that, obtain the equations for light propagation in such a universe.

Finally, in Chapter 4, I present my numerical results for light propagation in such a universe and discuss their significance in the context of some of the previous analytical analyses.

1.4 A note on units and notation

I use a comma to denote partial derivative and an overdot to denote derivative with respect to the affine parameter λ. For example, $x_{,t} = \frac{\partial x}{\partial t}$ and $\dot{x} = \frac{dx}{d\lambda}$. Throughout this work I use natural units $c = G = 1$.

2 Gravitational lensing formalism

2.1 Mathematical preliminaries

The essence of General Relativity (GR) is very elegantly summarised by John Wheeler (Wheeler and Ford, 2000, pg.235) in a sentence: matter tells spacetime how to curve, and spacetime tells matter how to move.

The first half of this statement is quantified by the Einstein Field Equations (EFEs), which is the analogue of Poisson's equation in Newtonian gravity. They are a group of 10 coupled differential equations that describe the interaction between matter and geometry of spacetime, given by (in tensor notation)

$$G_{\mu\nu} + \Lambda g_{\mu\nu} = 8\pi T_{\mu\nu} \tag{2.1}$$

where $g_{\mu\nu}$ is the metric of spacetime, Λ is the cosmological constant, $G_{\mu\nu}$ is the Einstein tensor and $T_{\mu\nu}$ is the energy-momentum tensor. The energy momentum tensor on the right hand side is a source term that encodes how matter is distributed in the universe, and on the left hand side the Einstein tensor depends on the metric tensor, which describes the spacetime geometry. For a perfect pressureless fluid, the energy momentum tensor is

$$T^{\mu\nu} = \rho u^{\mu} u^{\nu} \tag{2.2}$$

where u^{μ} is the 4-velocity of the fluid.

If we solve Einstein's field equations, we can obtain the metric tensor $g_{\mu\nu}$, which encodes the spacetime geometry. The metric tensor then influences how a particle behaves in this spacetime, bringing us to the second part of the statement: spacetime tells matter how to move. Given a metric tensor $g_{\mu\nu}$, we can first write down the line element

$$ds^2 = g_{\mu\nu} dx^{\mu} dx^{\mu} \tag{2.3}$$

Equations of motion of a particle moving in this spacetime can then be derived by first considering the Lagrangian of this particle

$$\mathcal{L} = \sqrt{g_{\mu\nu}\frac{dx^\mu}{d\lambda}\frac{dx^\nu}{d\lambda}} \tag{2.4}$$

where λ is an affine parameter which increases monotonically along the particle's worldline and $x^\mu(\lambda)$ describes the trajectory of the particle. Between two spacetime points A and B, we want to maximize $\int_B^A L(x^\mu, \dot{x}^\mu)\, d\lambda$, so $\mathcal{L}$ satisfies the Euler-Lagrange (E-L) equations

$$\frac{\partial \mathcal{L}}{\partial x^\mu} - \frac{d}{d\lambda}\left(\frac{\partial \mathcal{L}}{\partial \dot{x}^\mu}\right) = 0. \tag{2.5}$$

From the E-L equations we arrive at the geodesic equation

$$\ddot{x}^\mu + \Gamma^\mu_{\alpha\beta}\dot{x}^\alpha\dot{x}^\beta = 0 \tag{2.6}$$

where an overdot represents a derivative with respect to the affine parameter λ, and Γ are the Christoffel symbols given by

$$\Gamma^\mu_{\alpha\beta} = \frac{1}{2}g^{\mu\rho}(g_{\rho\alpha,\beta} + g_{\rho\beta,\alpha} - g_{\alpha\beta,\rho}). \tag{2.7}$$

A freely moving particle always moves along a geodesic, which is a generalisation of the notion of "straight lines" to a curved spacetime. In addition, light, as a massless particle, travels along null geodesics, in contrast to timelike ones for massive particles. Therefore, all light trajectories have to satisfy the null condition

$$g_{\mu\nu}dx^\mu dx^\nu = 0. \tag{2.8}$$

The result is a handful of coupled differential equations that need to be solved to find the trajectory of light. Nevertheless, a common problem arising in cosmology stems from the fact that as soon as we depart from the simplest homogeneous models used by observational cosmologists, the task of finding solutions to null geodesics quickly becomes an intractable analytical problem. In our work, we instead use a numerical method to integrate the null geodesics to find the trajectory of the photon.

2.2 Derivation of bending angle in the Schwarzschild metric

It is useful to first revise gravitational lensing in a universe without Λ, in a Schwarzschild metric, which is well understood. This will form the basis for our comparison with a universe that includes Λ.

Spacetime outside a spherically symmetric distribution of matter and vacuum everywhere else is described by the Schwarzschild metric, one of the first known solutions to Einstein's field equations. Its line element is given by

$$ds^2 = -\left(1 - \frac{2M}{r}\right)dt^2 + \left(1 - \frac{2M}{r}\right)^{-1} dr^2 + r^2(d\theta^2 + \sin^2\theta d\phi^2). \tag{2.9}$$

where M is the central mass.

Due to spherical symmetry, we can restrict ourselves to the equatorial plane $\theta = \pi/2$ without loss of generality. This metric is asymptotically flat as $r \to \infty$. We can then find the total deflection angle α experienced by light that comes in from $r = -\infty$, gets deflected, and travels on towards $r = +\infty$ as

$$\alpha = 2\int_{r_0}^{\infty} \left|\frac{d\phi}{dr}\right| dr - \pi \tag{2.10}$$

where r_0 is the distance of closest approach.

The static nature and spherical symmetry of the Schwarzschild metric implies that there are two constants of motion for any particle traveling in this geometry. These can be obtained through direct application of the E-L equation (Eq. 2.5), and we have

$$E = \left(1 - \frac{2M}{r}\right)\dot{t}, \tag{2.11a}$$

$$L = r^2\dot{\phi}. \tag{2.11b}$$

By applying the null condition (Eq. 2.8) on the metric, we obtain an expression for $\frac{d\phi}{dr}$

$$\frac{d\phi}{dr} = \pm\frac{1}{r^2}\sqrt{\frac{1}{\frac{1}{b^2} - \left(1 - \frac{2M}{r}\right)\frac{1}{r^2}}} \tag{2.12}$$

where $b = L/E$ is the impact parameter (since $\frac{d\phi}{dr} = \dot{\phi}/\dot{r}$). Integrating this (for a detailed derivation see Keeton and Petters, 2005), we obtain an expression for the bending angle α as a series expansion in M/r_0. This series, to third order in M/r_0, is as follows:

$$\alpha = 4\frac{M}{r_0} + \left(-4 + \frac{15\pi}{4}\right)\left(\frac{M}{r_0}\right)^2 + \left(\frac{122}{3} - \frac{15\pi}{2}\right)\left(\frac{M}{b}\right)^2. \tag{2.13}$$

This can be easily converted to a series in M/b instead of M/r_0, which is usually done in literature, since a relation between b and r_0 can be derived in a series expansion by setting $\dot{r} = 0$, giving (Keeton and Petters, 2005)

$$r_0 = b\left[1 - \frac{M}{b} - \frac{3}{2}\left(\frac{M}{b}\right)^2 - 4\left(\frac{M}{b}\right)^3\right]. \tag{2.14}$$

This relation can then be used to rewrite the expansion in terms of $\frac{M}{b}$ to give us

$$\alpha = 4\frac{M}{b} + \frac{15\pi}{4}\left(\frac{M}{b}\right)^2 + \frac{128}{3}\left(\frac{M}{b}\right)^3. \tag{2.15}$$

and indeed many authors use the impact parameter to discuss the bending of light in Schwarzschild spacetime (Wald, 2010; Misner et al., 2017; Butcher, 2016). However, it has been pointed out previously by other authors (Ishak, Rindler, Dossett, et al., 2008; Hammad, 2013; Lebedev and Lake, 2013) that in the non-zero Λ case, the definition of the impact parameter is no longer independent of Λ and becomes questionable due to the fact that spacetime is no longer asymptotically flat.

In this work we will use another constant of the motion for the non-zero Λ case, and for consistency we will use that parameter here as well so that a fair comparison can be made, even though the Schwarzschild case does not include a cosmological constant.

We can define another constant of the motion R_u which corresponds to the unperturbed trajectory of light (see Fig. 1), which is related to r_0 by (see Eq. 6 of Ishak, Rindler, Dossett, et al. (2008) and Eq. 3 of Butcher (2016)).

$$\frac{1}{r_0} = \frac{1}{R_u} + \frac{M}{R_u^2} + \frac{3M^2}{16R_u^3} \tag{2.16}$$

where I have added a subscript u to differentiate it from the Kottler coordinate R in the next chapter. Using this relation and applying it to Eq. 2.13, we can get a series expansion in M/R_u, which, up to third order, is given by

$$\alpha = 4\frac{M}{R_u} + \frac{15\pi}{4}\left(\frac{M}{R_u}\right)^2 + \frac{401}{12}\left(\frac{M}{R_u}\right)^3. \tag{2.17}$$

There are 3 length quantities that are typically used in Schwarzschild lensing: the distance of closest approach r_0, the impact parameter b, and the parameter of the unperturbed trajectory R_u. They are related to each other through Eq. 2.14 and Eq. 2.16, and their related series expansions are respectively given by Eq. 2.13, Eq. 2.15 and Eq. 2.17. The coefficient of the leading order term is the same for all three but they differ on higher order terms in the series expansion. Many gravitational lensing anayses done on the Schwarzschild metric are only concerned with the leading order term, and hence

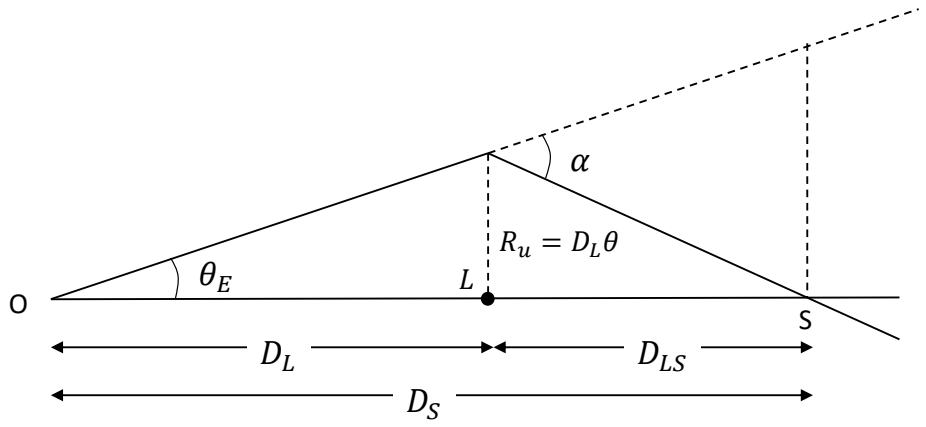

Figure 1: Diagram of gravitational lensing, where the lens, observer, and source are collinear.

use these three lengths somewhat interchangeably. But in this project we are interested in corrections at the second order or higher, and the distinction becomes important. In the subsequent section of the report, we will be using the series expansion in M/R_u (Eq. 2.17).

As mentioned previously, Rindler and Ishak (2007) proposed a different expression for α. The expression was later refined for a Swiss-cheese universe (Ishak, Rindler, Dossett, et al., 2008), and I will state it here (in our notation) for easy comparison:

$$\alpha_{\text{Ishak}} = 4\frac{M}{R_u} + \frac{15\pi}{4}\left(\frac{M}{R_u}\right)^2 + \frac{305}{12}\left(\frac{M}{R_u}\right)^3 - \frac{\Lambda R_u R_h}{3}, \tag{2.18}$$

where R_h is the boundary of the hole in static coordinates in the Swiss-cheese model. The Λ-term is negative, and they postulate that the cosmological constant attenuates lensing.

2.3 Lensing observables

A significant part of the conflict in literature comes from the question of which quantities in lensing are observable, and whether these observable quantities are ultimately affected by the presence of the cosmological constant. Therefore we aim to stick with strictly observable quantities.

We consider a simple picture where the observer, lens, and source are aligned, as shown in Fig. 1. Bending is assumed to happen at a single point above the lens, since the distance from the observer to the lens and source is assumed to be much larger than the distance of closest approach between the light ray and the lens. From this diagram we can easily, with some trigonometry, obtain the lens equation (Schneider et al., 1992)

$$D_S \theta_E = D_{LS} \alpha \tag{2.19}$$

where α is the bending angle as previously derived, D_S is the angular diameter distance from observer to source, D_{LS} is the angular diameter distance from lens to source, and θ_E is known as the Einstein angle. R_u can also be expressed in terms of the observable quantities $R_u = D_L \theta_E$, where D_L is the angular diameter distance from observer to the lens.

With this in mind, we can begin looking at the Swiss-cheese model, and look to apply this formalism in such a universe.

3 Description of the Swiss-cheese model

3.1 Spacetime patches

Swiss-cheese (SC) models were first introduced by Einstein and Straus (1945) to investigate the gravitational field of a mass well described by the Schwarzschild metric but embedded in a non-Minkowski background spacetime. Such a model is contructed by removing a comoving sphere from the homogeneous background and replacing it with an inhomogeneous mass distribution (see Fig. 2). In this case, we use a mass distribution that is vacuum everywhere except for a point mass at the centre. In principle, since the sphere is comoving, multiple spheres can be inserted in the cheese as long as they are initially non-overlapping. In our model, only one hole is needed to model the lens. This stitching of two metrics on the cheese-hole boundary is of course not arbitrary, and matching conditions will impose restriction on the parameters of the two metrics. This will be discussed in detail in the following sections.

There are several reasons why this model was chosen. First, this is an exact solution of Einstein's equations which preserves the global dynamics, and hence it will allow us to properly investigate the higher order corrections that have been oft-debated in literature. Secondly, by putting observers in the homogeneously expanding "cheese", it accounts for observers moving with the Hubble flow, which is a common objection to Rindler and Ishak's use of a static metric (Park, 2008; Khriplovich

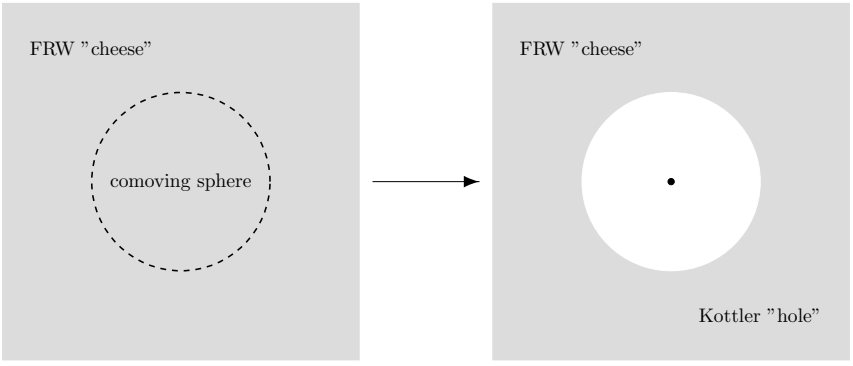

Figure 2: Construction of a Swiss-cheese model

and Pomeransky, 2008; Simpson et al., 2010; Butcher, 2016). Lastly, this model also takes the finite range of the mass into account by confining the influence of the central mass to the size of the hole.

Light propagation in SC models has been extensively studied (Szybka, 2011; Vanderveld et al., 2008; Fleury, 2014), but not particularly so in the subject of the Λ dependence on gravitational lensing. Some of the areas that Swiss-cheese models have been commonly used include investigating the effect of local inhomogeneities on luminosity-redshift relations (Kantowski, 1969; Fleury et al., 2013) and studying fluctuations in redshift and distance of the cosmic microwave background (Bolejko, 2009; Valkenburg, 2009; Bolejko, 2011).

A significant difference between the Swiss-cheese model and what is used in conventional gravitational lensing, as described in the previous section, is that in the Swiss-cheese, the bending happens only inside the hole, whereas in conventional lensing, the mass is superimposed on the FRW background and has infinite range. In the Swiss-cheese model, due to the boundary conditions, all bending is truncated once the light ray leaves the hole, and outside the hole the light ray travels as if the hole does not exist. Therefore even in the $\Lambda = 0$ case, we would expect a slightly smaller bending angle in the Swiss-cheese than predicted in conventional lensing, even though this difference is small.

Kantowski et al. (2010) did analytical calculations in estimating the bending angle in the Swiss-cheese model in flat space (see Eq. 32 of Kantowski et al. (2010)). This prediction, together with the conventional lensing prediction (Eq. 2.17) and the Rindler and Ishak prediction (Eq. 2.18), are the theoretical models that we will be comparing our numerical results against.

3.1.1 Friedmann-Robertson-Walker geometry

Outside the hole, geometry is described by the Friedmann-Robertson-Walker (FRW) metric, the simplest homogeneous and isotropic model of the universe. Its line element, in spherical polar coordinates, is given by (Wald, 2010)

$$ds^2 = -dt^2 + a(t)^2\left(\frac{dr^2}{1-kr^2} + r^2 d\Omega^2\right) \tag{3.1}$$

where $d\Omega^2 = d\theta^2 + \sin^2\theta d\phi^2$ is the metric on a 2-sphere, $a(t)$ is the varying scale factor of the universe, and k represents the curvature of space. This is the line element for a homogeneous and expanding universe with general spatial curvature. There are 3 possibilities for the value of k, each implying a different geometry of the universe:

- $k = 0$: The universe is flat and Euclidean.
- $k > 0$: The universe has positive spatial curvature and is closed

- $k < 0$: The universe has negative spatial curvature and is open.

The scale factor a parametrises the relative expansion of the universe, such that the relationship between physical distance and comoving distance between two points at a certain cosmic time t is given as

$$d_{\text{physical}} = a(t) d_{\text{comoving}}. \tag{3.2}$$

The scale factor also satisfies the Friedmann equation

$$H^2 \equiv \left(\frac{1}{a}\frac{da}{dt}\right)^2 = \frac{8\pi G\rho}{3} + \frac{\Lambda}{3} - \frac{k}{a^2} \tag{3.3}$$

where ρ is the energy density of a pressureless fluid and H is the Hubble parameter.

It is common to introduce the cosmological parameters, where a subscript 0 refers to quantities evaluated today:

$$\Omega_m = \frac{8\pi G\rho_0}{3H_0^2},\ \Omega_\Lambda = \frac{\Lambda}{3H_0^2},\ \Omega_k = -\frac{k}{a_0^2 H_0^2} \tag{3.4}$$

and rewrite the Friedmann equation as

$$H^2 = H_0^2\left[\Omega_m\left(\frac{a_0}{a}\right)^3 + \Omega_k\left(\frac{a_0}{a}\right)^2 + \Omega_\Lambda\right] \tag{3.5}$$

where the Ω terms are commonly known as density parameters, evaluated at the present day. In the absence of radiation, they obey the relation

$$\Omega_m + \Omega_\Lambda + \Omega_k = 1. \tag{3.6}$$

In a flat universe, space is Euclidean and $\Omega_k = 0$.

3.1.2 Kottler geometry

In this project we use a Kottler condensation in the Swiss-cheese for the central lensing mass. This is described by a Kottler metric (Kottler, 1918), which is the extension of the famous Schwarzschild metric to include a cosmological constant, given by

$$ds^2 = -f(R)dT^2 + \frac{dR^2}{f(R)} + R^2 d\Omega^2 \tag{3.7}$$

with

$$f(R) = 1 - \frac{2M}{R} - \frac{\Lambda R^2}{3}, \tag{3.8}$$

where M is the mass of the central object. Unlike the FRW, this metric describes a static spacetime.

3.2 Matching conditions

Two geometries can be matched across the boundary to form a well defined spacetime if and only if they satisfy the Darmois-Israel junction conditions (Darmois, 1927; Israel, 1966). These conditions dictate that the first and second fundamental forms of the two metrics must match on the matching hypersurface Σ, that is, both metrics must induce (i) the same metric, and (ii) the same extrinsic curvature.

3.2.1 Continuity of the induced metric

We match the FRW and Kottler metrics on a surface of a comoving 2-sphere, Σ, which is defined by $r = r_h =$ constant in FRW coordinates and $R = R_h(T)$ in Kottler coordinates.

The induced metric is the quantity

$$h_{ab} = g_{\alpha\beta} j_a^\alpha j_b^\beta \tag{3.9}$$

where j_a^α is defined as

$$j_a^\alpha = \frac{\partial \bar{X}^\alpha}{\partial \sigma^a}. \tag{3.10}$$

Here we have introduced X^α to represents coordinates of the original metric. We define σ^a to be natural intrinsic coordinates for Σ, and $\bar{X}^\alpha(\sigma^a)$ is the parametric equation of the hypersurface.

More concretely, using the coordinates defined previously in Eq. 3.1, these quantities are, for the FRW,

$$X^\alpha = \{t, r, \theta, \phi\} \tag{3.11a}$$
$$\sigma^a = \{t, \theta, \phi\} \tag{3.11b}$$
$$\bar{X}^\alpha(\sigma^a) = \{t, r_h, \theta, \phi\}. \tag{3.11c}$$

Similarly, in the Kottler region, we have

$$X^\alpha = \{T, R, \theta, \phi\} \tag{3.12a}$$
$$\sigma^a = \{T, \theta, \phi\} \tag{3.12b}$$
$$\bar{X}^\alpha(\sigma^a) = \{T, R_h(T), \theta, \phi\}. \tag{3.12c}$$

Using these definitions, the 3-metric induced by the FRW geometry on Σ is

$$ds^2_\Sigma = -dt^2 + a^2(t) r^2 d\Omega^2, \tag{3.13}$$

while the induced metric on the Kottler metric is

$$ds^2_\Sigma = -\kappa^2(T) dT^2 + R_h^2(T) d\Omega^2, \tag{3.14}$$

where

$$\kappa \equiv \sqrt{\frac{f^2[R_h(T)] - \left(\frac{dR_h(T)}{dT}\right)^2}{f[R_h(T)]}}. \tag{3.15}$$

Equating the components of Eq. 3.13 and Eq. 3.14, we obtain the following:

$$R_h(T) = a(t) r, \tag{3.16}$$

$$\frac{dt}{dT} = \kappa(T). \tag{3.17}$$

These two relationships relate the radial and time coordinates of the two metrics respectively.

3.2.2 Continuity of the extrinsic curvature

The second condition equates extrinsic curvature of the two geometries. By definition, the extrinsic curvature K_{ab} of a hypersurface is given by

$$K_{ab} = n_{\alpha;\beta} j_a^\alpha j_a^\beta \tag{3.18}$$

where n_μ is the unit vector normal to Σ, j is as defined previously in Eq. 3.10, and the semicolon notation ';' denotes a covariant derivative, for example, $n_{\alpha;\beta} = \nabla_\beta n_\alpha$. For any vector V^ν, the covariant derivative is defined as

$$\nabla_\mu V^\nu = \partial_\mu V^\nu + \Gamma^\nu_{\mu\rho} V^\rho. \tag{3.19}$$

For a hypersurface defined by a function $q = 0$, the unit vector normal to it is

$$n_\mu = \frac{q_{,\mu}}{\sqrt{g^{\alpha\beta} q_{,\alpha} q_{,\beta}}}. \tag{3.20}$$

In our case $q = r - r_h$ in FRW coordinates and $q = R - R_h(T)$ in Kottler coordinates. For example, the unit vector in the FRW region is trivial to calculate, and we get $n_\mu^{(\mathrm{FRW})} = \delta^r_\mu / a$. Applying this formula, the extrinsic curvature induced by the FRW geometry is

$$K_{ab} dx^a dx^b = \frac{a(t) r}{\sqrt{1 - kr^2}} d\Omega^2 \tag{3.21}$$

while the extrinsic curvature induced by the Kottler geometry is

$$K_{ab} dx^a dx^b = \frac{1}{\kappa} \left[\frac{d^2 R_h}{dT^2} + \frac{f'}{2f} \left(f^2 - 3 \left(\frac{dR_h}{dT} \right)^2 \right) \right] dT^2 + \frac{R_h f}{\kappa} d\Omega^2 \tag{3.22}$$

where $f' = \partial f / \partial R$, and all quantities are evaluated at $R = R_h(T)$.

Equating the components of Eq. 3.21 and Eq. 3.22, we obtain

$$\frac{R_h f}{\kappa} = \frac{a(t) r}{\sqrt{1 - kr^2}} \tag{3.23}$$

and

$$\frac{d^2 R_h}{dT^2} + \frac{f'}{2f} \left[f^2 - 3 \left(\frac{dR_h}{dT} \right)^2 \right] = 0. \tag{3.24}$$

The second equation is provided for completeness although it is not needed for subsequent derivations.

3.2.3 Consequences on properties of the hole

Combining Eq. 3.23 with Eq. 3.15, we can eliminate κ. We can also replace dR_h/dT using the relation obtained in Eq. 3.16, since

$$\frac{dR_h}{dT} = \frac{d(ar)}{dT} = \frac{da}{dt} \frac{dt}{dT} r. \tag{3.25}$$

where da/dt is given by the Friedmann equation 3.3. Following through with the algebra, we arrive at the somewhat intuitive result that both regions must have the same cosmological constant Λ and

that the Kottler hole has to be mass compensating, meaning the enclosed mass M has to equal the mass excised from the FRW background:

$$M = \frac{4\pi}{3}\rho a^3 r_h^3. \tag{3.26}$$

From the junction conditions the rate of expansion of the hole in static coordinates can also be obtained. By combining Eq. 3.15 and Eq. 3.23, we get an expression for dR_h/dT

$$\frac{dR_h}{dT} = f(R_h)\sqrt{1 - \frac{f(R_h)}{1 - kr_h^2}}. \tag{3.27}$$

The last thing we need from the boundary conditions is to relate the tangent vectors between the two metrics. The continuity of the metric, imposed by the first junction condition, implies that the connection does not diverge across the boundary. Therefore, light is not deflected as it crosses the boundary and we just need to convert the components of the tangent vector between the two coordinate systems. To obtain $\dot{R}$ in terms of FRW tangent vectors $\dot{r}$ and $\dot{t}$, we differentiate Eq. 3.16 and substitute da/dt with the Friedmann equation Eq. 3.3. Keeping in mind the boundary conditions, we get an expression for $\dot{R}$. The angular coordinates and angular tangent vectors are unchanged when moving from the Kottler to FRW coordinates, and vice versa. With $\dot{R}$ and $\dot{\phi}$, $\dot{T}$ then can be easily obtained from the null condition Eq. 2.8. The result is

$$\dot{T} = \frac{\dot{t}}{f}\sqrt{1 - kr^2} + \frac{a\dot{r}}{f\sqrt{1 - kr^2}}\sqrt{\frac{2M}{ar} - kr^2 + \frac{\Lambda}{3}a^2r^2} \tag{3.28a}$$

$$\dot{R} = \dot{t}\sqrt{\frac{2M}{ar} - kr^2 + \frac{\Lambda}{3}a^2r^2} + a\dot{r} \tag{3.28b}$$

$$\dot{\phi} = \dot{\phi} \tag{3.28c}$$

$$\dot{\theta} = \dot{\theta} \tag{3.28d}$$

where for completeness I have also given the trivial relations between the angular tangent vectors. The quantities above are all evaluated at the boundary of the hole. This result is given for flat space in Schücker (2009) and Fleury et al. (2013), but here it has been extended to allow for arbitrary spatial curvature. The reverse transformation is easily obtained by inverting the Jacobian from above.

In summary, given a FRW spacetime with pressureless matter and a cosmological constant Λ, a spherical hole, whose geometry is described by the Kottler metric, can be constructed which contains a constant mass $M = 4\pi\rho a^3 r_h^3/3$ at its centre. The geometry resulting from combining the two metrics at the boundary is an exact solution of the Einstein field equations. Applying the boundary

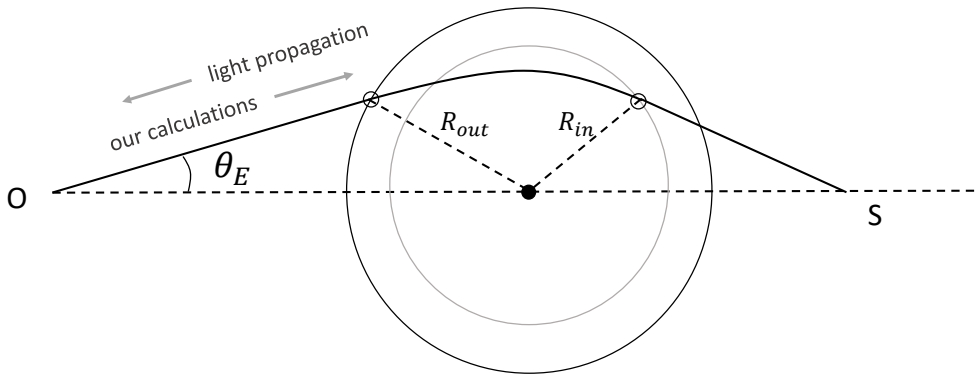

Figure 3: A diagram of how a light ray propagates through the Swiss-cheese. Our calculations are done in the opposite direction of propagation. Due to the expansion of the universe, the physical size of the hole will be larger when the light exits the hole compared to when it entered.

conditions, we can obtain all the necessary transformations needed for continuation of light propagation at the boundary.

3.3 Light propagation

We propagate a light ray backwards from observer to source by solving the geodesic equation (Eq. 2.6). In reality, the light ray travels from source to observer, but our calculations proceed in the opposite direction since we want to take the current observer position and observation event as the initial condition. The observer is placed in the FRW region, where we start propagating the light ray. The mass of the lensing object is fixed and consequently so is the size of the hole. The light ray is started off with an Einstein angle θ_E, travels through the FRW region, encounters the Kottler hole which deflects its trajectory, and returns to the FRW region again (see Fig. 3. In the Swiss-cheese model, all the bending occurs only in the Kottler hole and is truncated once light leaves the hole.

We begin by fixing the lens redshift, since it is the redshift that is directly observable and not the radial coordinate r. From the lens redshift, we can then calculate the radial coordinate and angular diameter distance to the lens.

In the FRW, assuming $a_0 = 1$, we can calculate the angular diameter distance D_L for a given lens redshift z_L as (Hogg, 1999)

$$D_L = D_A(z_L) = \frac{1}{1+z_L} S_k\left(\frac{1}{H_0}\int_0^{z_L} \frac{dz}{\sqrt{\Omega_m(1+z)^3 + \Omega_k(1+z)^2 + \Omega_\Lambda}}\right) \tag{3.29}$$

where we define the function $S_k(x)$

$$S_k(x) = \begin{cases} |k|^{-1/2} \sin(\sqrt{|k|}x) & k > 0 \\ x & k = 0 \\ |k|^{-1/2} \sinh(\sqrt{|k|}x) & k < 0 \end{cases} \tag{3.30}$$

and its inverse function

$$S_k^{-1}(x) = \begin{cases} |k|^{-1/2} \sin^{-1}(\sqrt{|k|}x) & k > 0 \\ x & k = 0 \\ |k|^{-1/2} \sinh^{-1}(\sqrt{|k|}x) & k < 0 \end{cases} \tag{3.31}$$

In terms of the angular diameter distance, the radial coordinate is given by

$$r_L = (1 + z_L) D_L. \tag{3.32}$$

Therefore, as we vary Λ, r_L is expected to change since we fix z_L. We then place the lens at the origin and observer at a radial coordinate of $r = r_L$ and $\phi = \pi$.

Numerical integration is done with the `scipy.integrate.solve_ivp` function in Python (Jones et al., 2014), which uses an explict Runge-Kutte method of order 5 (Dormand and Prince, 1980). The solver uses an adaptive step size, and the intersection between the light ray and the point of entry and exit of the hole are found with the classic Brent's method (Brent, 2013), a root-finding algorithm.

3.3.1 FRW region

The light ray begins from the observer in the FRW region. The starting tangent angle θ_E is fixed, and the initial tangent vectors are set such that $\theta_E = \tan^{-1}(\sqrt{1 - kr^2} r\dot{\phi}/\dot{r})$. We place the lens at the origin and take the observer to be at an azimuthal angle of $\phi = \pi$.

Null geodesics govern the trajectory of the light ray. Without loss of generality, we can take $\theta = \pi/2$ to simplify the geodesic equations. Due to spherical symmetry, the FRW has a conserved quan-

tity $L = a^2 r^2 \dot{\phi}$ that corresponds to the angular momentum of the photon. In terms of the conserved quantity, the null geodesic equations are

$$\dot{t} = -\sqrt{\frac{a^2 \dot{r}^2}{1 - kr^2} + a^2 r^2 \dot{\phi}} \tag{3.33a}$$

$$\ddot{r} = (1 - kr^2) r \dot{\phi}^2 - \frac{kr\dot{r}^2}{1 - kr^2} - \frac{2a_{,t}}{a} \dot{r}\dot{t} \tag{3.33b}$$

$$\dot{\phi} = \frac{L}{a^2 r^2} \tag{3.33c}$$

which, when combined with the Friedmann equation (Eq. 3.5), fully determine the light's path. The negative sign on $\dot{t}$ is due to the fact that we are propagating the light backwards in time. We can then solve these differential equations numerically and stop the integration once the light ray reaches the boundary of the hole, which is defined by $r_h = \text{constant}$. We call this intersection event $\mathcal{E}_{\text{out}}$, since this is where the light, traveling from the source to observer in the opposite direction of our numerical calculations, *leaves* the hole.

In the particular case of Euclidean geometry ($k = 0$), the coordinates of the event $\mathcal{E}_{\text{out}}$ can be calculated analytically. To do this, we first rewrite the flat metric in terms of the conformal time η, defined by $d\eta = dt/a(t)$, as

$$ds^2 = a^2(\eta)\left(-d\eta^2 + dr^2 + r^2 d\Omega^2\right). \tag{3.34}$$

We can then write down the following system of equations in Cartesian coordinates x^i_{out}, in terms of the hole radius r_h and Cartesian position of the observer x^i_0:

$$\delta_{ij}(x^i_{\text{out}} - x^i_h)(x^j_{\text{out}} - x^j_h) = r_h^2 \tag{3.35a}$$

$$x^i_{\text{out}} = x^i_0 + (\eta_0 - \eta_{\text{out}}) d^i \tag{3.35b}$$

where d^i is the unit vector representing direction of travel. For a given Einstein angle θ_E, in Cartesian coordinates we have

$$d = \frac{1}{\sqrt{(\dot{r}\cos\phi - r\sin\phi\dot{\phi})^2 + (\dot{r}\sin\phi + r\cos\phi\dot{\phi})^2}} \begin{pmatrix} \dot{r}\cos\phi - r\sin\phi\dot{\phi} \\ \dot{r}\sin\phi + r\cos\phi\dot{\phi} \end{pmatrix} \tag{3.36}$$

The final thing we need is to recover the scale factor from the conformal time. From Eq. 3.35, we can obtain the value of η_{out}, since we can arbitrarily set $\eta_0 = 0$. We take $a_0 = 1$ at the observer, so the conformal time η is related to a by

$$\eta_{\text{out}} = \frac{1}{H_0} \int_1^{a_{\text{out}}} \frac{1}{a^2 \sqrt{\Omega_m / a^3 + \Omega_\Lambda}}. \tag{3.37}$$

where H_0 is the current value of the Hubble parmeter. Since η increases monotonically with a, we did a simple binary search to find the value of a_{out} that produced η_{out} to the required level of accuracy.

The above calculation only applies for flat space, and in arbitrarily curved space, we do the full numerical integration to obtain the conditions at $\mathcal{E}_{\text{out}}$.

3.3.2 Conversion from FRW region to Kottler region at $\mathcal{E}_{\text{out}}$

From the FRW coordinates and tangent vectors, we can first obtain the starting coordinate R_{out} from Eq. 3.16. The angular coordinates remain the same in both coordinate systems. We are free to set $T_{\text{out}} = 0$ since we are not concerned with the amount of time taken by the light, only the trajectory.

The initial tangent vectors to start off the Kottler integration can be obtained from the Jacobian derived in the previous section (Eq. 3.28).

3.3.3 Kottler region

Inside the hole, the staticity and spherical symmetry of the Kottler metric imply the existence of two conserved quantities, $E = f(R)\dot{t}$ and $L = R^2\dot{\phi}$, which correspond to the energy and angular momentum of the photon respectively. The null condition, after rearranging to make $\dot{R}$ the subject, reads

$$\dot{R} = \pm \sqrt{E^2 - \frac{L^2}{R^2}\left(1 - \frac{2M}{R} - \frac{\Lambda R^2}{3}\right)}. \tag{3.38}$$

The $\pm$ before square root on the right hand side is troublesome for numerical computations because it would become necessary to determine a point to switch signs for $\dot{R}$. To circumvent that, we can differentiate the equation obtained from the null condition to get a second order differential equa-

tion in R. Combining that with the conserved quantities, we have the following equations which fully determine the light trajectory in Kottler space:

$$\dot{T} = \frac{E}{f(R)} \tag{3.39a}$$

$$\ddot{R} = \frac{L^2(R - 3M)}{R^4} \tag{3.39b}$$

$$\dot{\phi} = \frac{L}{R^2}. \tag{3.39c}$$

Note that the second order differential equation in R now has no dependence on Λ, which is the aforementioned conventional argument pioneered by Islam (1983) for why Λ does not directly contribute to lensing.

At the same time that the light ray is moving through the Kottler hole, the hole boundary is also changing in the static coordinates, with an expansion rate governed by Eq. 3.27. This equation needs to be integrated simulataneously with the null geodesic equations in order to find the point that the light ray intersects with the hole again. We call this event $\mathcal{E}_{\text{in}}$, again to emphasize the fact that this is where light enters the hole, although the propagation is done in the opposite direction.

3.3.4 Conversion from Kottler region to FRW region at $\mathcal{E}_{\text{in}}$

Conversion from the Kottler to FRW region is simply the reverse of the transformations stated in Section 3.3.2. We set $t_{\text{in}} = 0$ since we are not concerned with the path time.

3.3.5 Back in the FRW region

Once we get back to the FRW region, we continue using FRW null geodesics (Eq. 3.33) to propagate the light and stop once we reach the axis. The coordinate at which it crosses the axis is then recorded.

In flat space, numerical integration here is no longer necessary, since there will be no more bending in this region. Thus the intersection of the light path with the axis can be calculated from the tangent vector directly once light exits the Kottler hole.

3.3.6 Converting raw radial coordinates to angular diameter distances

Our aim is to compare our results against the cosmological lens equation (Eq. 2.19), using strictly observable quantities. Gravitational lensing analysis is usually done with us (the observer) at the origin, but in our model we have placed the lens at the origin instead out of convenience. Therefore we

take extra care when converting from raw radial coordinates back into observable angular distances. By an extension of the redshift formula (Eq. 3.29), we can get the angular diameter distance between two arbitrary points given their respective radial coordinates (Peacock, 1999)

$$D_{AB} = \frac{a_0 S_k(S_k^{-1}(r_B) - S_k^{-1}(r_A))}{1 + z_B} \tag{3.40}$$

Applying this formula and remembering that we place the observer at $(r, \phi) = (r_L, \pi)$, we can use our final numerical coordinate at $(r, \phi) = (r_{LS}, 0)$ to get D_S and D_{LS}:

$$D_S = \frac{S_k(S_k^{-1}(r_{LS}) + S_k^{-1}(r_L))}{1 + z_S} \tag{3.41a}$$

$$D_{LS} = \frac{r_{LS}}{1 + z_S} \tag{3.41b}$$

With this, we now have all the formulation needed to carry out the numerical integration and also to translate the numerical results into observable quantities.

We also extend this model beyond a Kottler hole to a general static mass distribution, by replacing the Kottler metric by a LTB metric with pressure and deriving the null geodesics again in this spacetime. The quantities and results for the LTB metric are presented in Appendix A.

4 Results and discussion

In order to test the robustness of the numerical integration routine, we checked that the results agreed with the FRW bending angle Eq. 2.17 to at least within 0.1%. We were also able to reproduce the results presented in Schücker (2009) to the stated precision.

A graph of results when we keep the lensing mass M constant and vary Ω_Λ can be seen in Fig. 4. On the y-axis, we plot the deviation of D_S/D_{LS} as a fraction of the standard FRW lensing case (found by substituting Eq. 2.17 into the lens equation 2.19), in order to put them on the same scale. We plot the fractional deviation of D_S/D_{LS} instead of D_S or D_{LS} alone since they both depend on the numerical result. That is, if we define $s = D_S/D_{LS}$ then we are plotting the quantity $s_{\text{numerical}}/s_{\text{FRW}} - 1$.

Numerical errors are estimated by varying the tolerance of the integrator. For a certain tolerance level, we group the results obtained from the vicinity of tolerance levels together and find the variance in the numerical result in that range to get a crude estimation of the numerical error. Fig. 5 shows how the raw r_{LS} coordinate obtained from the integration varies with the relative tolerance level. As is expected, the precision increases as the tolerance level is reduced. For a relative tolerance of 2×10^{-14}, a conservative estimate obtained by grouping results between $r_{\text{tol}} = 2 \times 10^{-14}$ and 2×10^{-13} yields a fractional error of 10^{-8}.

Our results follow the trend of Kantowski's predictions most closely, with a gap that reduces towards higher Λ. A possible explanation of this gap can be found by examining the neglected higher order term in Kantowski's predicted bending angle, $\mathcal{O}(2M/r_0 + \Lambda r_0^2)^{5/2}$. When $\Lambda = 0$, the ratio of this term to his leading order $(4M/r_0^2)\cos^3\tilde{\phi}_1$ term is of the same order of magnitude as the fractional deviation of our numerical results from Kantowski's predictions. As is expected, our results deviate less from Kantowski's as this ratio decreases, as shown in Fig. 6.

From the graph, we can see that even for the $\Lambda = 0$ case there is an offset between the numerical Swiss-cheese result and the FRW prediction. Qualitatively, this is due to the fact that conventional lensing analyis assumes a mass superimposed on the homogeneous background, and this mass has infinite range. However, in the Swiss-cheese model, the influence of the mass is limited, and bending stops once it leaves the Kottler hole. This is the main effect that Kantowski quantified in his paper Kantowski et al. (2010). This then begs the question of which model is a more accurate description

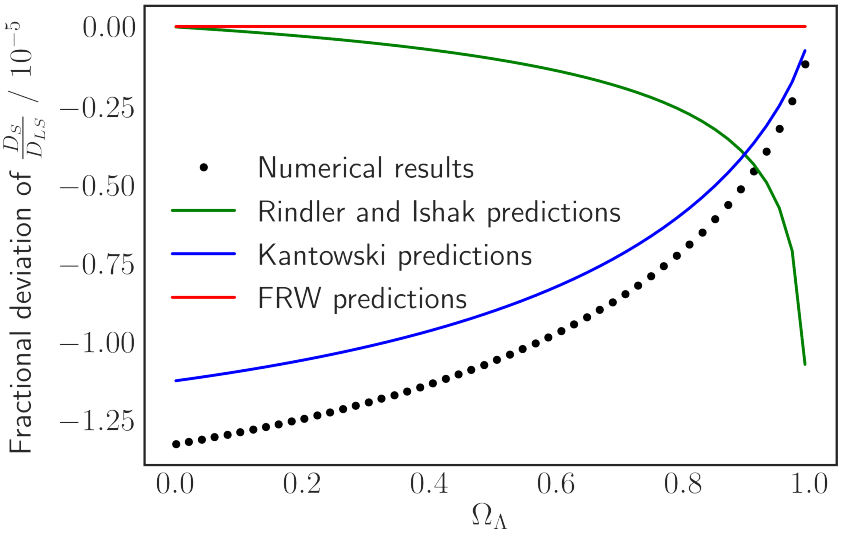

Figure 4: These are the results when we keep the mass constant and vary Λ. The fractional deviations from the expected result in FRW are plotted (Eq. 2.17 and Eq. 2.19). The green curve is the Rindler & Ishak predictions while the blue curve is Kantowski's prediction. Black points are our numerical results. The starting conditions for this are $z_{\text{lens}} = 0.5$ and $\theta_E = 1''$, with Ω_Λ varying between 0 and 0.99. We use $M = 10^{13} M_\odot$ and $H_0 = 70\,\text{km}\,\text{s}^{-1}\,\text{Mpc}^{-1}$.

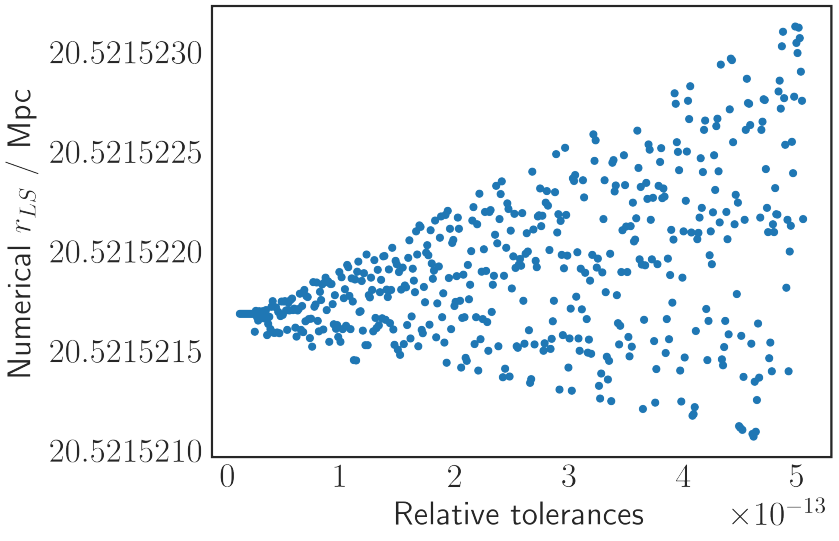

Figure 5: Plot of how the numerical result r_{LS} varies with the relative tolerance for $\Omega_\Lambda = 0$.

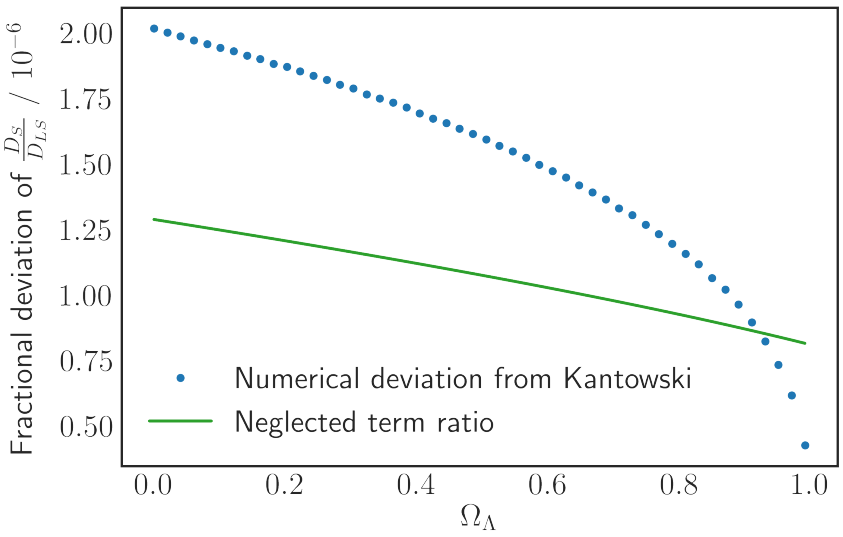

Figure 6: A plot of the absolute value of fractional numerical deviation from Kantowski's predictions, compared with the ratio of the higher order neglected term in Kantowski's calculation to his leading order term. They follow the same trend downwards, so it is a likely explanation that the difference is caused by the neglected higher order term.

of our physical universe, but this is not our primary concern. We are primarily concerned about whether Λ has an influence on this effect.

There are a few different factors at play here. In discussing the results of this numerical integration, let us take a step back to look at the specific parts of ray-tracing that have a Λ-dependence. These are:

1. The size of the hole. This is governed by Eq. 3.26. In flat space, increasing Ω_Λ implies decreasing Ω_m, which corresponds to the matter density of the universe. If we are to keep the mass constant, the hole size would have to increase as we increase Ω_Λ.

2. The rate of expansion of the hole in static Kottler coordinates, given by Eq. 3.27.

3. The Jacobian at the boundary, given by Eq. 3.28.

The first effect does not seem to be a truly direct Λ effect, merely a side effect that in a flat universe, changing Ω_Λ must imply a change in matter density, but ultimately, it is the size of the hole that is the true determining factor in this effect.

Therefore we look into keeping the hole size constant while varying Λ. The results for this are shown in Fig. 7, for the case of flat space. If the hole size is kept constant, then the mass will have to change with Ω_Λ. In this case, the comoving size of the hole was fixed at $2.60\,\mathrm{Mpc}$, which corresponds to a mass of $10^{13} M_\odot$ at $\Omega_\Lambda = 0$. The lens redshift was kept at $z_L = 0.5$ and the Einstein angle was set to be $1''$.

There is a difference between numerical results and Kantowski's predictions similar to the previous result that decreases with increasing Ω_Λ. This was plotted in Fig. 8 and indeed as we expect, the magnitude of the neglected higher-order term in his calculation follow the same general trend.

If we extend the integration for a universe with arbitrary curvature, then it is possible to fix both mass and r_h, but it would involve changing the curvature to compensate for the change in Λ. However, from the previous chapter, the curvature k affects the rate of expansion of the Kottler hole and also enters into the Jacobian at the boundary as well, so intuitively one would expect k to also have an effect on the bending angle in a Swiss-cheese model, though this effect has not been explored fully in literature (Kantowski's calculation Kantowski et al. (2010) only applies for flat space).

We have plotted the result of varying curvature to account for the change in Λ in Fig. 9. However, the results imply that the correction from curvature is even bigger than the Λ-effect, and hence it is unlikely to be useful.

Unfortunately, there is no way to keep both curvature and matter density constant while varying Λ, so we cannot truly isolate the effect of Λ. Ultimately, to compensate for a change in Λ, one has to vary either matter density or curvature, or both. In a Swiss-cheese model, both factors are expected to affect the lensing observables to some extent. Given the limited literature on the effect of curvature on lensing in the Swiss-cheese model, and the much larger deviations resulting from curvature based on our numerical simulations (Fig. 9), I would postulate that the variation of matter density has a smaller and better studied effect on lensing, and it is this we should vary such that the influence of Λ becomes most apparent. Moreover, current cosmological observations (Planck Collaboration et al., 2016; Hinshaw et al., 2013; de Bernardis et al., 2000) suggest quite convincingly that the Universe is spatially flat, and therefore looking at the case of $\Omega_k = 0$ is most appropriate.

Hence Fig. 7 is the graph of most significance. From the graph we can see that while there is a clear trend when varying Λ, this is smaller than that in Fig. 4, since the effect of different hole radius is eliminated. Similar to Fig. 4, there is an offset even when $\Lambda = 0$, due to the truncation of bending at the hole boundary.

Instead of comparing against the conventional FRW results, it is also instructive to compare the numerical results against the $\Lambda = 0$ point also obtained from numerical simulations, in a crude attempt to eliminate the effect at $\Lambda = 0$. These fractional deviations are even smaller than the deviations from the FRW result, at the order of 10^{-6}. These are 10 to 100 times smaller than second order mass terms, which are routinely neglected.

It was also pointed out by Butcher (2016) that there is an unavoidable ambiguity when determining the distances D_L, D_{LS}, and D_S. In this work we have used *unlensed* distances, that is, the distances were calculated as if the lens did not exist, when in reality the angular diameter distances are

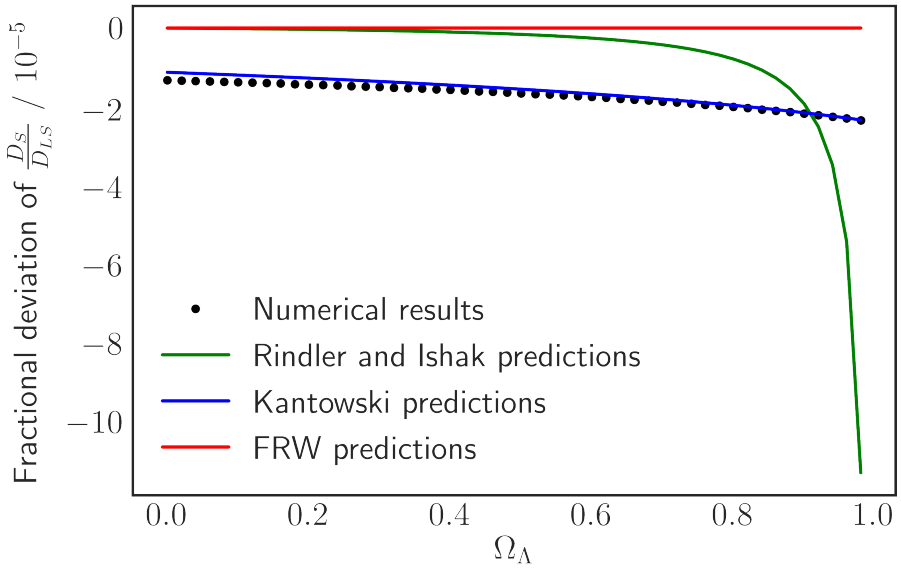

(a) $\Omega_\Lambda = 0$ to 0.99

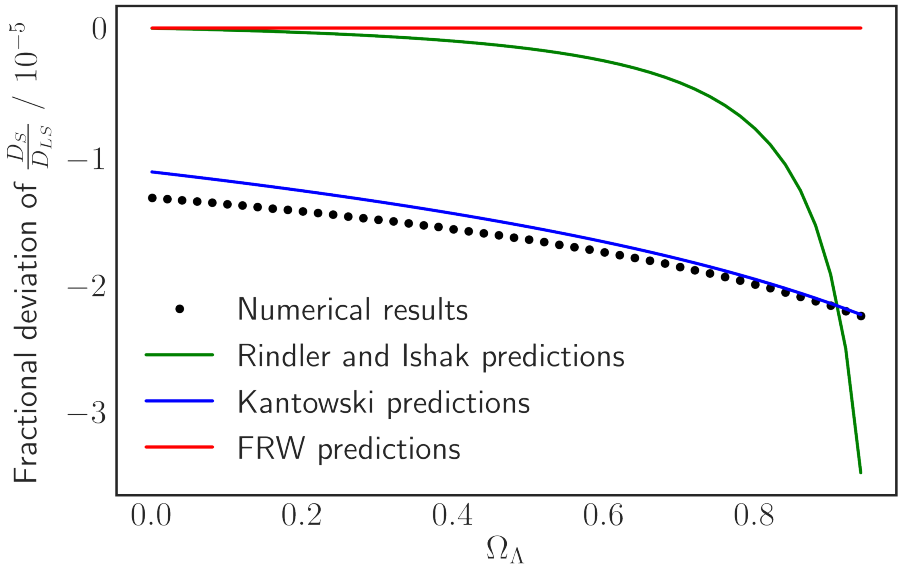

(b) $\Omega_\Lambda = 0$ to 0.95

Figure 7: Results of the numerical simulation in flat space when r_h is kept constant instead of M. The comoving size of the hole was fixed at 2.60 Mpc. This is the size such that at $\Omega_\Lambda = 0$, $M = 10^{13} M_\odot$. The left figure contains the full range from $\Omega_\Lambda = 0$ to 0.99, whereas the right figure is the slightly zoomed in version after removing two of the rightmost points, to make the differences at lower Ω_Λ more apparent.

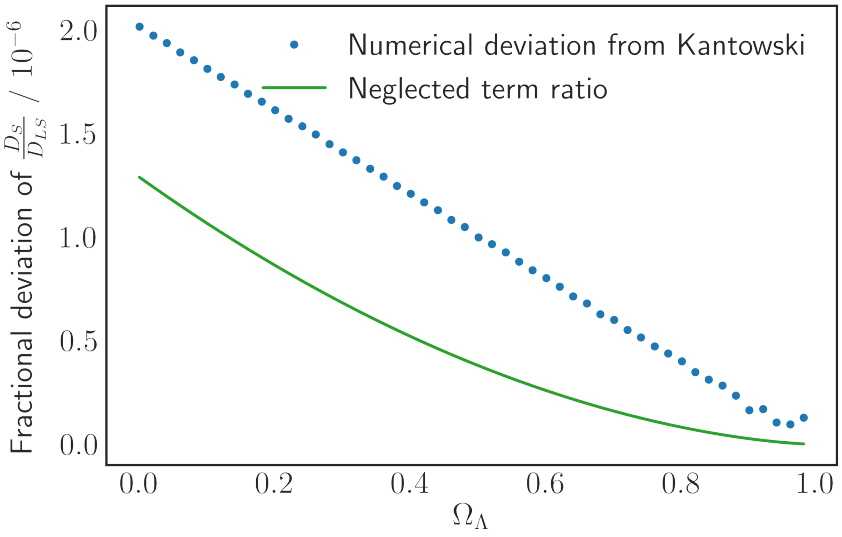

Figure 8: A plot of the fractional deviation of numerical results from Kantowski's predictions, together with the ratio of the higher order term magnitude neglected in his calculations to his leading order term.

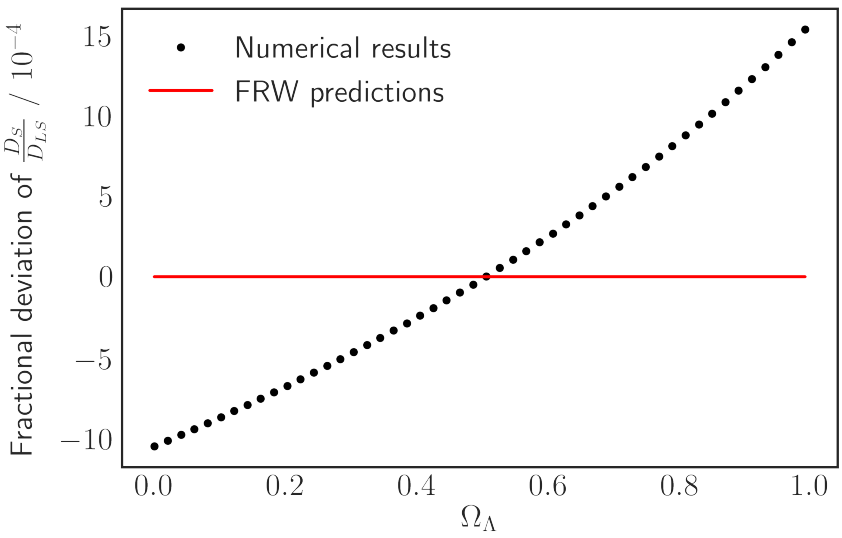

Figure 9: Plot of the results when Ω_m was kept constant at 0.5, $\Omega_\Lambda = 0$ to 0.99 and Ω_k was used to compensate for the change in Ω_Λ. The parameters used are $z = 0.5$, $M = 10^{13} M_\odot$. The numerical deviation is much bigger than the Rindler & Ishak prediction and Kantowski prediction.

necessarily modified by the existence of the lens. According to Butcher's calculations, the fractional uncertainty arising from using unlensed distances is given by

$$\frac{\delta D}{D} = \mathcal{O}\left(\frac{M}{\Lambda r^2}\right) \tag{4.1}$$

For $z_L = 0.5$, $M = 10^{13} M_\odot$, and $\Omega_\Lambda = 0.7$, we obtain a fractional uncertainty of about 10^{-9}, which is much smaller than the magnitude that we are considering.

5 Conclusion

In this work, we examined gravitational lensing in a Swiss-cheese model that has an embedded Kottler hole. We numerically integrated null geodesics in such a universe piecewise and calculated lensing observables from the numerical results. These results were compared with predictions by Rindler & Ishak and Kantowski. Our results agree most with Kantowski's predictions, with a small varying gap that can be explained by the presence of higher order terms not considered in Kantowski's results.

However, it is difficult to truly isolate the effect of Λ, since a change in Λ *must* involve a change in either Ω_m or Ω_k, and it is not clear at the outset which quantity should be kept constant as we turn up Λ. We looked into case where spatial curvature compensates for the change in Λ, but from our results it appears that Ω_k has a much larger effect than Λ on lensing observables in the Swiss-cheese model, so we focused on interpreting results from a spatially flat Universe.

We kept the hole size constant while varying Λ to eliminate any effect coming from the size of the hole that might be considered a Λ effect. Even so, Λ appears to have an effect on the lensing observables, although this effect is small—smaller than the size of the second order term in M/R_u, which is routinely neglected.

A last thing to note about our work is that its applicability of course hinges on the validity of the model used, but this can be said of most scientific work. The Swiss-cheese model has been used in other areas in cosmology not without success, as described in the introductory section of 3.

5.1 Future work

Our work is focused solely on the collinear case, in which the source, lens and observer are aligned, but it is straightforward to generalise beyond this restriction.

The case with curvature was somewhat glossed over, since curvature appeared to have a much larger influence than Λ, and most work done on embedded lens in a Swiss-cheese have been in a spatially flat universe. While it is not the focus of this report, it might be worthwhile to look into the corrections from curvature needed in a Swiss-cheese model. With better knowledge on the effect of curvature on lensing in such a model, it would be easier to isolate the Λ effect in gravitational lensing and facilitate more effective comparison between the curved results and the spatially flat case.

Lastly, it might be useful to extend this sytematic analysis beyond the Swiss-cheese model, possibly with the adoption of a different metric; after all, in our physical universe galaxies are not exactly completely spherical structures walled-off at a radius that varies strictly with its mass. Appendix A considers a more realistic (but still static) mass distribution, but it still operates in the Swiss-cheese framework. However, I believe this work to be a good starting point in quantifying the effect of the cosmological constant on lensing observables.

A Generalized static mass distribution with the LTB metric

In this section we generalize the model from a point mass vacuole to a vacuole with an arbitrary static mass distribution. In order to do that, the Kottler metric has to be replaced with another metric.

We use the Lemaître-Tolman-Bondi (LTB) model (Tolman, 1934; Bondi, 1947; Lemaître, 1933), which is the most general spherically symmetric solution of Einstein's field equations without the assumption of spatial homogeneity. It has the FRW model as a special sub-case. The model was originally a dust model but was later extended to include pressure (Lasky and Lun, 2006), and this pressure term is needed to achieve a static system. The metric is given by

$$ds^2 = A(R)^2 dT^2 - \frac{dR^2}{f(R)} - R^2 d\Omega^2. \tag{A.1}$$

where $f(R)$ is given by Eq. 3.8. This is very similar to the Kottler metric except that the mass term in $f(R)$ is now a function of radius and there is an new term $A(R)$. Solving the EFEs for this metric yield the usual Tolman-Oppenheimer-Volkoff (TOV) equations (Tolman, 1939; Oppenheimer and Volkoff, 1939) for a static stellar interior, which give us the variation of $A(R)$ with R as

$$A_{,R} = -A\frac{P_{,R}}{\rho + P} \tag{A.2}$$

where P changes with R as

$$P_{,R} = \frac{\rho + P}{2\left(1 - \frac{2M}{R} - \frac{\Lambda R^2}{3}\right)R}\left(\frac{2\Lambda R^2}{3} - 8\pi P R^2 - \frac{2M}{R}\right) \tag{A.3}$$

and M, ρ are quantities that depend on R.

On the matching surface, the metric reduces to the Kottler metric. Therefore the boundary conditions given in Chapter 3 remain valid. In addition, there are boundary conditions on P and A, given by

$$P = 0 \tag{A.4}$$

$$A^2 = 1 - \frac{2M}{R} - \frac{\Lambda R^2}{3}. \tag{A.5}$$

The null geodesic equations expressed in terms of these quantities are

$$\dot{T} = \frac{E}{A(R)^2} \tag{A.6a}$$

$$\ddot{R} = \frac{E^2}{2}\left(\frac{f_{,R}}{\alpha^2} - \frac{2f\alpha_{,R}}{\alpha^3}\right) - \frac{L^2}{2}\left(\frac{f_{,R}}{R^2} - \frac{2f}{R^3}\right) \tag{A.6b}$$

$$\dot{\phi} = \frac{L}{R^2} \tag{A.6c}$$

where E and L are constants of the motion, and $f_{,R}$ is given by

$$f_{,R} = \frac{2M}{R^2} - 8\pi\rho R - \frac{2\Lambda R}{3}. \tag{A.7}$$

These equations combined with Eq. A.2 and Eq. A.3 determine the trajectory of light through this metric.

We use the NFW profile (Navarro et al., 1996) for the mass distribution to model a physically motivated galaxy. In this profile the density is

$$\rho(R) = \frac{\rho_0}{\frac{R}{R_s}\left(1 + \frac{R}{R_s}\right)^2} \tag{A.8}$$

where R_s is the scale radius. Given a radius R_{max}, the total mass is given by

$$M_{\text{total}} = 4\pi\rho_0\left[\ln\left(\frac{R_s + R_{\text{max}}}{R_s}\right) - \frac{R_{\text{max}}}{R_s + R_{\text{max}}}\right] \tag{A.9}$$

and since total mass is fixed then we can find ρ_0. R_s can also be expressed in terms of the virial radius R_{vir} and the halo concentration parameter c

$$R_s = \frac{R_{\text{vir}}}{c}. \tag{A.10}$$

If we assume that the extent of the mass distribution is very small compared to the distances between the source, lens, and observer, then this justifies the thin-screen approximation, which states that the mass distribution of the lens can be treated as if it were an infinitely thin mass sheet per-

pendicular to the line-of-sight. Since we have a spherically symmetric mass distribution, the lensing mass is given by

$$M(R_u) = 2\pi \int_0^{R_u} \Sigma(R) R dR \tag{A.11}$$

where R_u is as defined in Chapter 3 and $\Sigma(R)$ is the projected surface density

$$\Sigma(R) = \int \rho(R, z) dz \tag{A.12}$$

where z is in the direction connecting the lens, observer, and source. Eq. A.11 represents the mass contained within a cylinder of radius R_u, with an axis parallel to the ray and passing through the centre of the lens.

Substituting in the density for a NFW mass profile, the lensing mass M_p for a given R_u is given by (Eq. 43 of Łokas and Mamon (2001))

$$M_p(R) = \frac{M_{\text{total}}}{\ln\left(\frac{R_s+R_{\text{max}}}{R_s}\right) - \frac{R_{\text{max}}}{R_s+R_{\text{max}}}} \left[\frac{C^{-1}(R_{\text{vir}}/R)}{|R^2/R_{\text{vir}}^2 - 1|^{1/2}} + \ln\left(\frac{R}{2R_{\text{vir}}}\right) \right] \tag{A.13}$$

where C^{-1} is the function

$$C^{-1}(x) = \begin{cases} \cos^{-1}(x) & R > R_s \\ \cosh^{-1}(x) & R < R_s \end{cases} \tag{A.14}$$

If the light ray does not pass through the mass at all, or if we supply a point mass for the mass distribution, then the result reduces to that of a Kottler Swiss-Cheese. This was used to check the robustness of the code.

We use $c = 10$ which roughly corresponds to the masses of bright galaxies (Łokas and Mamon, 2001). Density was truncated at $R_{\text{max}} = r_h/2$ to take into account the volume change of the hole in static coordinates as the universe expands. We set $R_{\text{vir}} = r_h/100$. For these parameters, the density, mass, and pressure functions are plotted in Fig. 10.

Fig. 11 shows the results of the numerical simulations in flat space when compared with the conventional, Rindler & Ishak, and Kantowski's predictions.

The results show the same general trend as the Kottler case, except now the there is a bigger discrepancy between the conventional result and the numerical result. This is likely the error induced by the thin-screen approximation. Frittelli and Kling (2011) found that the thin lens approximation when applied to the NFW mass profile produced an error of similar magnitude.

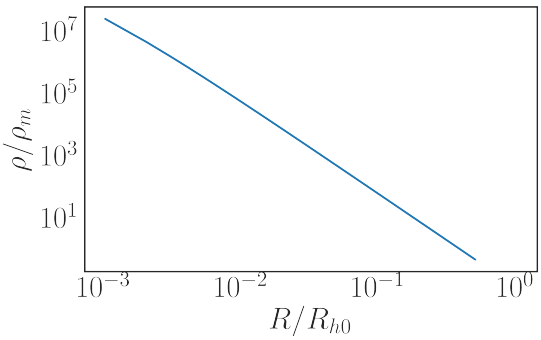

(a) Density

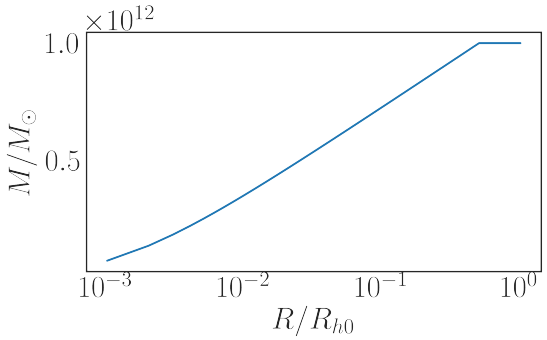

(b) Mass

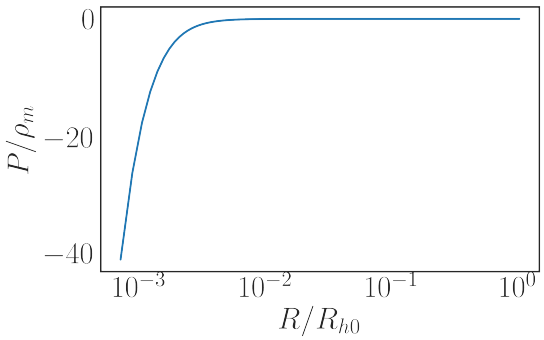

(c) Pressure

Figure 10: Plot of the mass, density, and pressure functions for $\Omega_\Lambda = 0$. The radial coordinate is expressed in terms of $R_{h0} = r_h$, the initial size of the Kottler hole. The density and pressure are expressed in terms of the density of the initial FRW density ρ_m. Density is truncated at $R = r_h/2$. We use $c = 10$ and $R_{\text{vir}} = r_h/100$

.

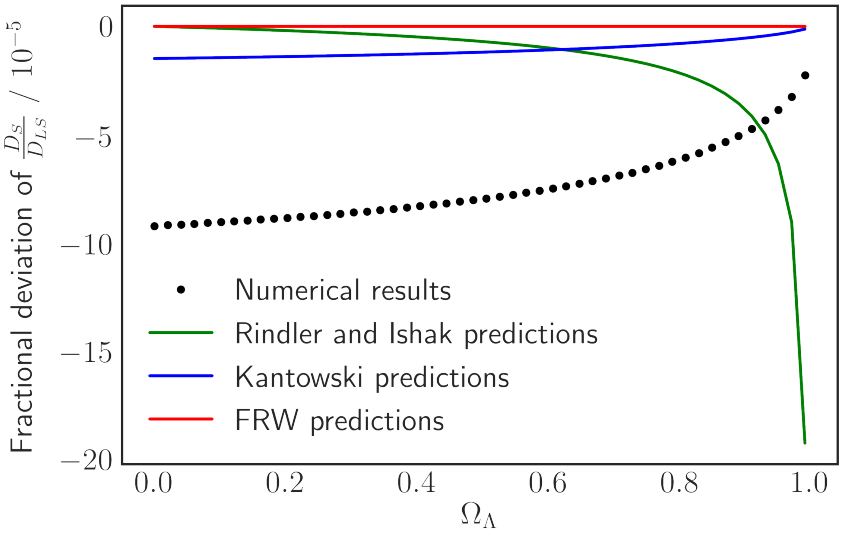

Figure 11: Results for the LTB model with parameters $c = 10$, $M_{\text{total}} = 10^{12} M_\odot$, $\theta_E = 0.5''$, $R_{\text{max}} = r_h/2$, $R_{\text{vir}} = r_h/100$. Numerical results are plotted as a fractional deviation from the conventional FRW lensing predictions, as are the Rindler & Ishak and Kantowski predictions.

References

Aghili, M. E., B. Bolen, and L. Bombelli (2017). "Effect of accelerated global expansion on the bending of light". *General Relativity and Gravitation* 49.1, p. 10.

Arakida, H. and M. Kasai (2012). "Effect of the cosmological constant on the bending of light and the cosmological lens equation". *Physical Review D* 85.2, p. 023006.

Beynon, E. (2012). "Testing gravity and dark energy with gravitational lensing". PhD thesis. University of Portsmouth.

Bhadra, A., S. Biswas, and K. Sarkar (2010). "Gravitational deflection of light in the Schwarzschild–de Sitter space-time". *Physical Review D* 82.6, p. 063003.

Bolejko, K. (2009). "The Szekeres Swiss Cheese model and the CMB observations". *General Relativity and Gravitation* 41.8, pp. 1737–1755.

Bolejko, K. (2011). "The effect of inhomogeneities on the distance to the last scattering surface and the accuracy of the CMB analysis". *Journal of Cosmology and Astroparticle Physics* 2011.02, p. 025.

Bondi, H. (1947). "Spherically symmetrical models in general relativity". *Monthly Notices of the Royal Astronomical Society* 107.5-6, pp. 410–425.

Brent, R. P. (2013). *Algorithms for minimization without derivatives*. Courier Corporation.

Butcher, L. M. (2016). "No practical lensing by Lambda: Deflection of light in the Schwarzschild–de Sitter spacetime". *Physical Review D* 94.8, p. 083011.

Carmeli, M. and T. Kuzmenko (2001). "Value of the cosmological constant: Theory versus experiment". *AIP Conference Proceedings*. Vol. 586. 1. AIP, pp. 316–318.

Darmois, G. (1927). *Les équations de la gravitation einsteinienne*. Gauthier-Villars.

de Bernardis, P. et al. (2000). "A flat Universe from high-resolution maps of the cosmic microwave background radiation". *Nature* 404.6781, p. 955.

Dormand, J. R. and P. J. Prince (1980). "A family of embedded Runge-Kutta formulae". *Journal of computational and applied mathematics* 6.1, pp. 19–26.

Einstein, A. and E. G. Straus (1945). "The influence of the expansion of space on the gravitation fields surrounding the individual stars". *Reviews of Modern Physics* 17.2-3, pp. 120–124.

Fleury, P. (2014). "Swiss-cheese models and the Dyer-Roeder approximation". *Journal of Cosmology and Astroparticle Physics* 2014.06, p. 054.

Fleury, P., H. Dupuy, and J.-P. Uzan (2013). "Interpretation of the Hubble diagram in a nonhomogeneous universe". *Physical Review D* 87.12, p. 123526.

Frittelli, S. and T. P. Kling (2011). "Accuracy of the thin-lens approximation in strong lensing by smoothly truncated dark matter haloes". *Monthly Notices of the Royal Astronomical Society* 415.4, pp. 3599–3608.

Hammad, F. (2013). "A note on the effect of the cosmological constant on the bending of light". *Modern Physics Letters A* 28.39, p. 1350181.

Hinshaw, G. et al. (2013). "Nine-year Wilkinson Microwave Anisotropy Probe (WMAP) Observations: Cosmological Parameter Results". *The Astrophysical Journal Supplement Series* 208.2, p. 19.

Hogg, D. W. (1999). "Distance measures in cosmology". *ArXiv Astrophysics e-prints*. arXiv: astro-ph/9905116.

Ishak, M., W. Rindler, and J. Dossett (2010). "More on lensing by a cosmological constant". *Monthly Notices of the Royal Astronomical Society* 403.4, pp. 2152–2156.

Ishak, M., W. Rindler, J. Dossett, et al. (2008). "A new independent limit on the cosmological constant/dark energy from the relativistic bending of light by galaxies and clusters of galaxies". *Monthly Notices of the Royal Astronomical Society* 388.3, pp. 1279–1283.

Islam, J. N. (1983). "The cosmological constant and classical tests of general relativity". *Physics Letters A* 97.6, pp. 239–241.

Israel, W. (1966). "Singular hypersurfaces and thin shells in general relativity". *Il Nuovo Cimento B (1965-1970)* 44.1, pp. 1–14.

Jones, E., T. Oliphant, and P. Peterson (2014). {*SciPy*}*: open source scientific tools for* {*Python*}. URL: http://www.scipy.org/.

Kantowski, R. (1969). "Corrections in the Luminosity-Redshift Relations of the Homogeneous Fried-Mann Models". *The Astrophysical Journal* 155, p. 89.

Kantowski, R., B. Chen, and X. Dai (2010). "Gravitational lensing corrections in flat ΛCDM cosmology". *The Astrophysical Journal* 718.2, p. 913.

Keeton, C. R. and A. O. Petters (2005). "Formalism for testing theories of gravity using lensing by compact objects: Static, spherically symmetric case". *Physical Review D* 72.10, p. 104006.

Khriplovich, I. B. and A. A. Pomeransky (2008). "Does the Cosmological Term Influence Gravitational Lensing?" *International Journal of Modern Physics D* 17.12, pp. 2255–2259.

Kottler, F. (1918). "Über die physikalischen grundlagen der Einsteinschen gravitationstheorie". *Annalen der Physik* 361.14, pp. 401–462.

Lake, K. (2002). "Bending of light and the cosmological constant". *Physical Review D* 65.8, p. 087301.

Lasky, P. D. and A. W. C. Lun (2006). "Generalized lemaitre-tolman-bondi solutions with pressure". *Physical Review D* 74.8, p. 084013.

Lebedev, D. and K. Lake (2013). "On the influence of the cosmological constant on trajectories of light and associated measurements in Schwarzschild de Sitter space". *ArXiv e-prints*. arXiv: 1308.4931 [gr-qc].

Lemaître, G. (1933). "L'Univers en expansion". *Annales de la Société Scientifique de Bruxelles* 53.

Łokas, E. L. and G. A. Mamon (2001). "Properties of spherical galaxies and clusters with an NFW density profile". *Monthly Notices of the Royal Astronomical Society* 321.1, pp. 155–166.

McVittie, G. C. (1933). "The mass-particle in an expanding universe". *Monthly Notices of the Royal Astronomical Society* 93, pp. 325–339.

Misner, C. W., K. S. Thorne, and J. A. Wheeler (2017). *Gravitation*. Princeton University Press.

Navarro, J. F., C. S. Frenk, and S. D. M. White (1996). "The structure of cold dark matter halos". *Symposium-international astronomical union*. Vol. 171. Cambridge University Press, pp. 255–258.

Oppenheimer, J. R. and G. M. Volkoff (1939). "On massive neutron cores". *Physical Review* 55.4, p. 374.

Park, M. (2008). "Rigorous approach to gravitational lensing". *Physical Review D* 78.2, p. 023014.

Peacock, J. A. (1999). *Cosmological physics*. Cambridge University Press.

Peebles, P. J. and B. Ratra (2003). "The cosmological constant and dark energy". *Reviews of modern physics* 75.2, p. 559.

Piattella, O. F. (2016). "Lensing in the McVittie metric". *Physical Review D* 93.2, p. 024020.

Planck Collaboration et al. (2016). "Planck 2015 results. XIII. Cosmological parameters". *Astronomy & Astrophysics* 594, A13.

Riess, A. G. et al. (2004). "Type Ia supernova discoveries at z> 1 from the Hubble Space Telescope: Evidence for past deceleration and constraints on dark energy evolution". *The Astrophysical Journal* 607.2, p. 665.

Rindler, W. and M. Ishak (2007). "Contribution of the cosmological constant to the relativistic bending of light revisited". *Physical Review D* 76.4, p. 043006.

Schneider, P., J. Ehlers, and E. E. Falco (1992). *Gravitational Lenses*. Springer.

Schücker, T. (2008). "Strong lensing with positive cosmological constant". *ArXiv e-prints*. arXiv: 0805.1630 [astro-ph].

Schücker, T. (2009). "Strong lensing in the Einstein–Straus solution". *General Relativity and Gravitation* 41.7, pp. 1595–1610.

Sereno, M. (2008). "Influence of the cosmological constant on gravitational lensing in small systems". *Physical Review D* 77.4, p. 043004.

Simpson, F., J. A. Peacock, and A. F. Heavens (2010). "On lensing by a cosmological constant". *Monthly Notices of the Royal Astronomical Society* 402.3, pp. 2009–2016.

Spergel, D. N. et al. (2003). "First-Year Wilkinson Microwave Anisotropy Probe (WMAP) Observations: Determination of Cosmological Parameters". *The Astrophysical Journal Supplement Series* 148.1, p. 175.

Szybka, S. J. (2011). "Light propagation in Swiss-cheese cosmologies". *Physical Review D* 84.4, p. 044011.

Tolman, R. C. (1934). "Effect of inhomogeneity on cosmological models". *Proceedings of the National Academy of Sciences* 20.3, pp. 169–176.

Tolman, R. C. (1939). "Static solutions of Einstein's field equations for spheres of fluid". *Physical Review* 55.4, p. 364.

Valkenburg, W. (2009). "Swiss cheese and a cheesy CMB". *Journal of Cosmology and Astroparticle Physics* 2009.06, p. 010.

Vanderveld, R. A., É. É. Flanagan, and I. Wasserman (2008). "Luminosity distance in "Swiss cheese" cosmology with randomized voids. I. Single void size". *Physical Review D* 78.8, p. 083511.

Wald, R. M. (2010). *General relativity*. University of Chicago press.

Wheeler, J. A. and K. Ford (2000). *Geons, black holes, and quantum foam: A life in physics*. WW Norton & Company.

Will, C. M. (1993). *Theory and Experiment in Gravitational Physics*. Cambridge University Press.